8th US National Technical Meeting
of the Combustion Institute
Hosted by University of Utah, Park City, Utah
May 19-22, 2013

Investigation of Non-Premixed Opposed Flow H_2/Air Laminar Flames using Coherent Anti-Stokes Raman Scattering (CARS)

Aman Satija,[1] Rajat D. Singh,[1] Sameer V. Naik,[1] and Robert P. Lucht[1]

[1]*School of Mechanical Engineering, Purdue University, West Lafayette, Indiana, USA*

Temperature profiles have been obtained along the centerline of non-premixed opposed flow H_2/Air flames using two counter-flow burners. The measurements were performed at varying strain rates but with fixed fuel and oxidizer composition to study the effect of strain rate on peak temperature and temperature profile shape. In addition, a qualitative study was conducted over a large range of strain rates, including unsteady regime, to investigate flame structure. Photographs of flames corresponding to some temperature profiles have also been included.

1. Introduction

Non-premixed, laboratory-scale, counterflow fuel/air flames decoupled from turbulence allow systematic investigation of the effects of strain rate and combustion chemistry upon flame structure. Niemann and co-workers [1] investigated the effect of pressure upon the structure and extinction of hydrogen counter-flow diffusion flames however, temperature measurements were obtained using R-type thermocouples; again non-intrusive temperature measurements would be valuable. Papas et al. [2] studied the extinction of non-premixed counter-flow flames of diluted hydrogen and air using laser Doppler velocimetry for pressures in the range of 0.5 to 1 atm. Experimental values of extinction strain rates agreed reasonably with those predicted using detailed kinetics. However, temperature measurements were not conducted. Most previous experimental studies of such counterflow flames have been performed using hydrocarbon fuels [3]. The data obtained from these experiments would serve as a useful comparison against CFD calculations such as done by Juniper et al. [4] who calculated the extinction limits of a counterflow diffusion flame between hydrogen and liquid oxygen with varying hydrogen inlet temperature using a one-dimensional numerical code. Another numerical simulation by Park et al. [5] investigated the effect of varying oxidizer inlet temperature and CO_2 dilution in the oxidizer stream upon the peak temperature in the flame and NO_x production rate. For the present experimental study we have employed N_2 vibrational CARS (VCARS) thermometry in two different counter-flow burners to systematically investigate the effect of varying strain rate upon the peak temperature and the shape of the temperature profiles along the nozzle centerline in non-premixed H_2/air flames.

2. Methods

Figure 1(a) shows the first counter-flow burner used for temperature measurements. It is also referred to as the "PIV-burner" in this paper since it was amenable to PIV measurements. The geometry of the nozzle is shown in Fig. 1(b). The burner has a 1 cm nozzle exit diameter and a 7.62 cm outside nozzle diameter. Each nozzle is constructed with a 5 cm diverging section, followed by a 9 cm straight section, and finally a 2 cm converging section. This design was used in order to obtain top-hat velocity profile for the reactants at the nozzle exit. The separation between the two nozzles for the PIV-burner was held constant at 1.1 cm. As this burner was designed for allowing PIV measurements it had no provision for co-flow. At higher strain rates the flames were found to be stable obviating the use of a co-flow anyway.

Figure 2 shows the second counter-flow burner used for temperature measurements. It is also referred to as the "coflow-burner" in this paper since it had a provision for co-flow. The coflow-burner was employed after a "secondary maximum" (undesirable distortion) was observed in the temperature profiles of the PIV-burner. This feature of the temperature profile is further discussed in the next section. The coflow-burner has an exit diameter of 1.9 cm, outer diameter of 5 cm and the nozzle separation was held constant at 13 mm. Unlike the PIV-burner, which had a tapering nozzle exit, this burner has a flat nozzle surface.

Temperature measurements were obtained using a broadband CARS system with a folded BOXCARS phase matching scheme [6]. The pump and probe beams were at 532 nm and the broadband Stokes beam with a bandwidth of 200 cm^{-1} was centered at 607 nm. The CARS signal was generated at 473 nm and subsequently detected using a CCD camera. Figure 3 shows the beam overlap at the probe volume. Both the burners were cooled using a chiller (Halco Products, Model 76607T) whose bath temperature was held constant at 298 K. At higher strain rates the flames developed an oscillatory behavior and were therefore, photographed using incoherent imaging (Canon Rebel XSi camera and a Canon EFS 55-250 mm lens).

3. Results and Discussion

Figures 4(a) and 5(a) show the raw Particle Image Velocimetry (PIV) images for non-reacting and reacting flows in the PIV-burner. In both cases pure H_2 and air were flowed from the bottom and top nozzle respectively with equal flow rates with a global strain rate of 225 s^{-1}. The details of the PIV experiment can be found in Satija et al. [7]. Velocity profiles along the nozzle centerline are also shown (Figs. 4(b) and 5(b)), the Y coordinate is the distance from the top nozzle and X coordinate is the horizontal distance across the burner. For the reacting flow, PIV data could not be obtained within the flame due to rapid volumetric expansion of the seeding particles; however, the results clearly show that flow velocity profile is flat over nearly 7 mm at the nozzle exit. The velocity information can be used as a boundary condition for realistic numerical simulations. Temperature profiles were obtained along the nozzle centerline at global strain rates of 250 s^{-1}, 347 s^{-1} and 444 s^{-1} respectively. The fuel consisting of 50% H_2 and 50% N_2 was flowed from the bottom nozzle and the oxidizer (air) was flowed from the top nozzle. In order to center the flames between the nozzles the volumetric flow rate from the fuel nozzle was slightly higher than the oxidizer nozzle. With an increase in strain rate, the peak temperature decreased and there was

narrowing of the width of the temperature profiles as seen in Figs 6-8. In addition, a "secondary maxima" was observed in the temperature profiles. This distortion of the profile seems to be related to heating of the oxidizer nozzle surface by the upwardly circulating combustion products. We obtained temperature measurements at 9 mm from the bottom nozzle for the 250 s^{-1} case and found sharp increase in the temperature outwards from the nozzle center as shown in Fig.9. This may explain the heating of the oxidizer nozzle surface.

At higher strain rates the flames began to exhibit oscillatory behavior and were therefore, studied qualitatively using incoherent imaging. Flames with more than 50% H_2 in the fuel stream remained stable even at strain rates of 1700 s^{-1} however flames with less than 35% H_2 in the fuel stream started to burn inside the nozzle. Figure 10 shows such a flame with 30% H_2 and 70% N_2 in the fuel stream. Interestingly, at the same fuel composition an additional flame "mode" could be observed over a range of global strain rates from 580 – 1350 s^{-1}. An example of this "bimodal" behavior at a global strain rate of 1350 s^{-1} is shown in Fig. 11(a) and 11(b). At lower strain rates mode 1 was more dominant and at higher strain rates mode 2 was more dominant. It was possible to switch between the two modes by simply blowing on the burner.

Due, to the presence of a secondary maximum in the temperature profile another counter-flow burner (coflow-burner) was used to investigate H_2/Air premixed flames. The oxidizer used was air and the fuel was a mixture of 30% H_2 and 70% N_2 with 48% and 52% of the total flow rate from the fuel and oxidizer nozzle respectively. No co-flow was used. The total flow rates were 15,30,45,53, and 60 slpm corresponding to a global strain rate of 67.8 s^{-1}, 135.7 s^{-1}, 203.5 s^{-1}, 239.7 s^{-1}, and 271.3 s^{-1} respectively. For the last condition the temperature profile was not obtained since the flame exhibited oscillatory behavior, however the peak temperature was noted. Figure 12 shows photograph of the flame in the burner at a global strain rate of 67.8 s^{-1} ; notice the upward pointing curvature of the flame. As the global strain rate was further increased, a secondary flame on the outside of this primary flame could be observed as shown in Fig. 13. For the flame shown in this figure the global strain rate was 239.7 s^{-1}. At the same strain rate another flame mode could be observed as shown in Fig. 14. Again, switching between the modes could be achieved by simply blowing on the flame. As the global strain rate was increased the second mode began to dominate and was the only relevant mode over strain rate of 300 s^{-1}. Figure 15 shows the flame structure at a strain rate of 420 s^{-1} ; notice the radial elongation of the flame with increasing strain rate.

Temperature profiles were also obtained along the nozzle centerline. Figures 16 through 19 show the temperature profiles for strain rates 67.8 s^{-1}, 135.7 s^{-1}, 203.5 s^{-1},and 239.7 s^{-1} respectively. There was a gradual decrease in peak temperature with increasing strain rate (shown in Fig. 20) along with a decrease in the width of the temperature profile. As the strain rate was increased, a secondary temperature rise was noted on the fuel side. We believe this happens because at higher flow rates, all of fuel is not burnt and forms the secondary flame. This idea is supported by a gradual increase in the luminosity of the secondary flame with increasing flow rates as shown in Figs 12 and 13.

4. Concluding Remarks

Two counter-flow burners were employed for investigating the effect of strain rate on non-premixed H_2/Air flames in the opposed-flow configuration. With both burners common trends are observed such as reduction in peak temperature and width of the temperature profile with increase in strain rate. Qualitative study shows two stable

modes for the flames when the fuel contained 30% H_2 and 70% N_2. In the PIV-burner this behavior was observed up to 1350 s^{-1}. The PIV-burner is advantageous because it allows measurements at higher strain rates due to a smaller diameter nozzle and the availability of PIV data in the burner will aid in numerical computations. However, the temperature profiles show a secondary maximum which will be further investigated using two-dimensional numerical modeling. A change in the PIV-burner design is being contemplated to "smoothen" the temperature profiles.

References

1) Niemann U. et al., "Effect of pressure on structure and extinction of near-limit hydrogen counterflow diffusion flames", Proc. of the Combustion Institute 34 (2013), 881-886.
2) Papas P. et al., "Effects of Pressure and Dilution on the Extinction of Counterflow Nonpremixed Hydrogen-Air Flames", Proc. of the Combustion Institute 25 (1995), 1333-1339.
3) Sennoun M.H. et al., "Laser Doppler Velocimetry Measurements in a Laminar Counter flow premixed double flame", IntJEnergeticMaterialsChemProp.v3.i1-6.440
4) Juniper M. et al., "The extinction limits of a hydrogen counterflow diffusion flame above liquid oxygen", Combustion and Flame 135 (2003), 87-96.
5) Park J. et al., "A Study on H_2-Air Counterflow Flames in Highly Preheated Air Diluted with CO_2", Energy & Fuels 2005, 19, 2254-2260.
6) Eckbreth A.C., "Laser diagnostics for Combustion Temperature and Species", Second Edition.
7) Satija A. et al., "Characterization of Counter-flow Methane-Air and Hydrogen-Air Flames using Stereo Particle Image Velocimetry (SPIV) and Coherent Anti-Stokes Raman Scattering (CARS)", presented at 7th US National Technical Meeting of the Combustion Institute, Atlanta,GA.

Figures

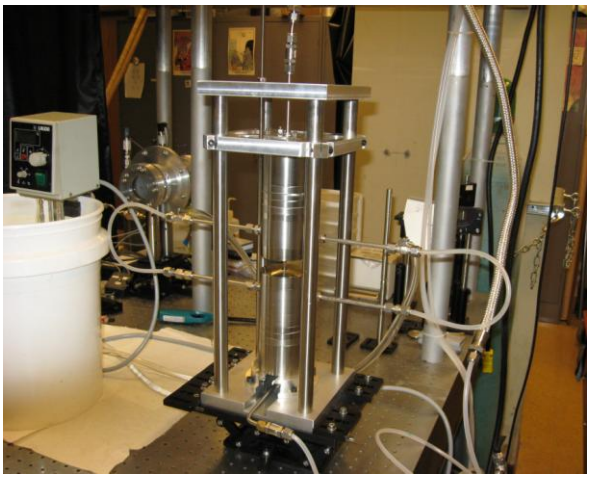

Figure 1: Counter-flow burner referred to as the PIV-burner.

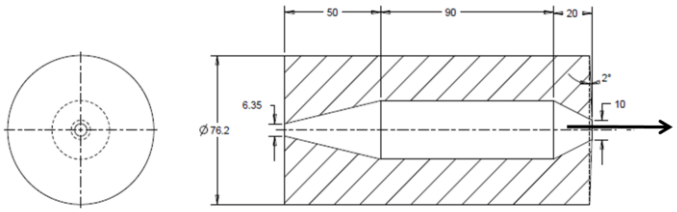

Figure 1b: Show the geometry of a single nozzle. All dimensions are in mm.

Figure 2: The 2nd counterflow burner referred to as the coflow-burner. The outer diameter of the burner = 5 cm.

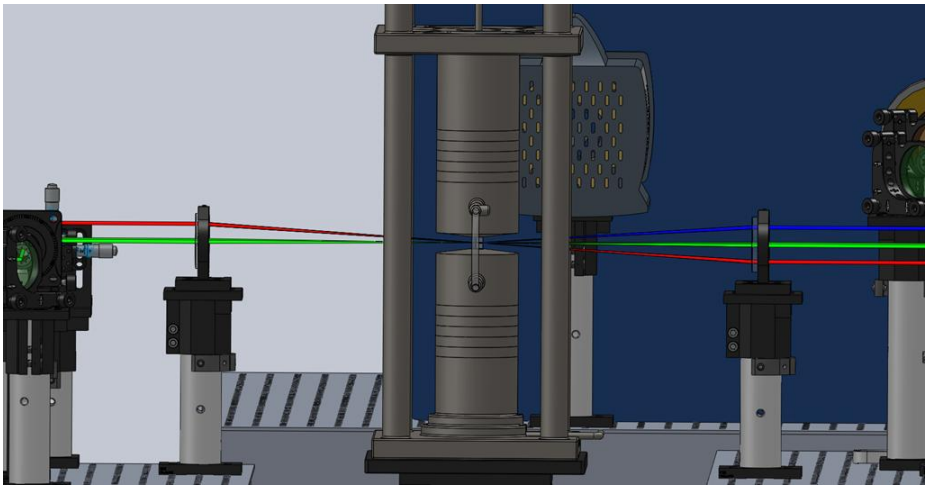

Figure 3: Here, the beams are propagating from left to right and are overlapping in the middle of the nozzles. The pump and the probe beam are at 532 nm, Stokes beam is shown in red and the generated N_2 VCARS signal is shown in blue.

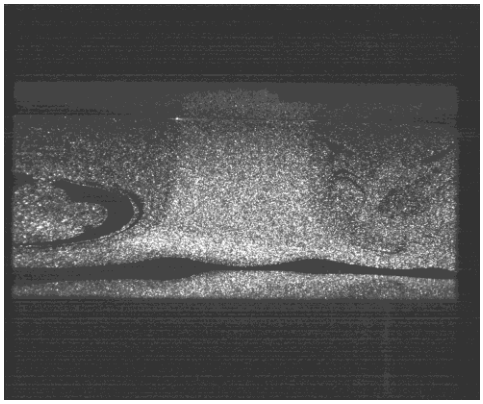

Figure 4a: Shows the raw PIV image for non-reacting flow condition. Note the re-circulating flow on the sides.

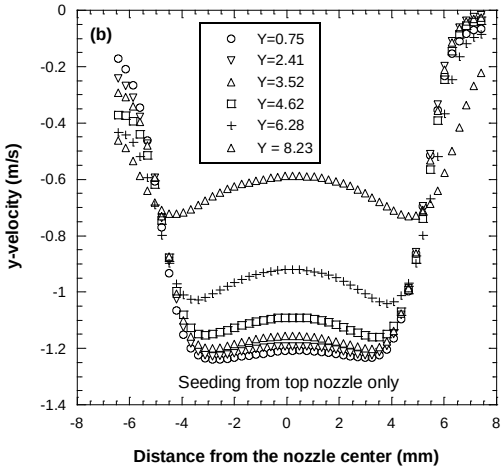

Figure 4b: Show the velocity profile for the non-reacting flow condition. The flow exiting the nozzle is at approximately at 1.3 ms^{-1} and the global strain rate is 225 s^{-1}. Note that the flow profile is nearly "top-hat" over 7.5 mm of the exit nozzle diameter.

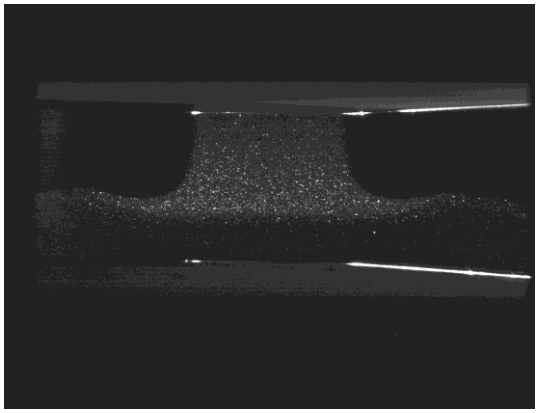

Figure 5a: Shows the raw PIV image for reacting flow condition. PIV data could not be obtained within the flame.

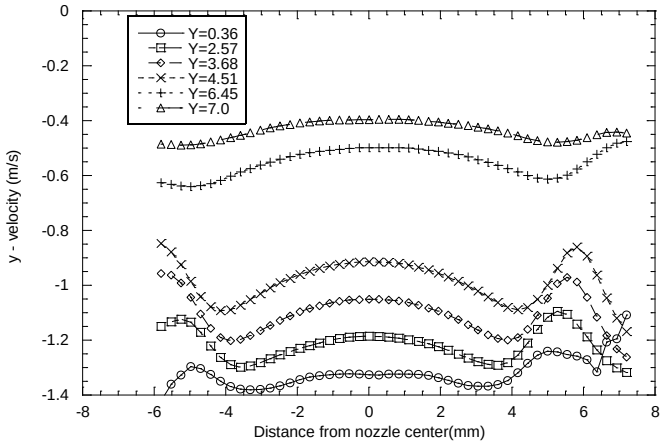

Figure 5b: Show the velocity profile for the reacting flow condition. The flow exiting the nozzle is at approximately at 1.3 ms^{-1} and the global strain rate is 225 s^{-1}. The flow profile shows more curvature for reacting flow than the non-reacting flow.

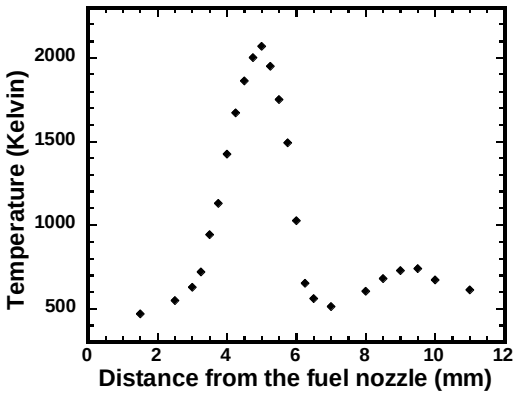

Figure 6: Temperature profile for strain rate in the PIV-burner at a global strain rate of 250 s^{-1}.

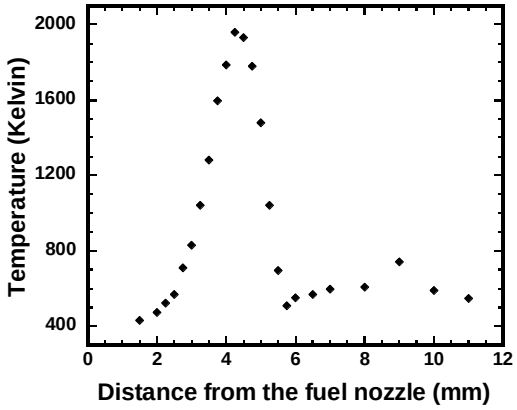

Figure 7: Temperature profile for strain rate in the PIV-burner at a global strain rate of 347 s^{-1}.

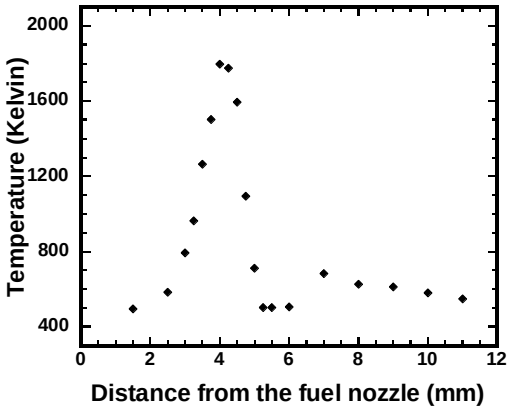

Figure 8: Temperature profile for strain rate in the PIV-burner at a global strain rate of 444 s^{-1}

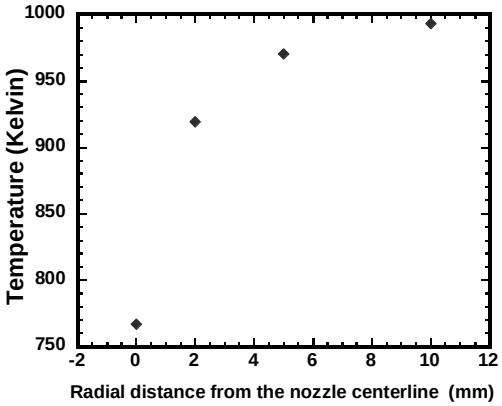

Figure 9: Temperature rises steeply in the radial direction from the nozzle centerline. Data obtained at 9 mm from the fuel nozzle.

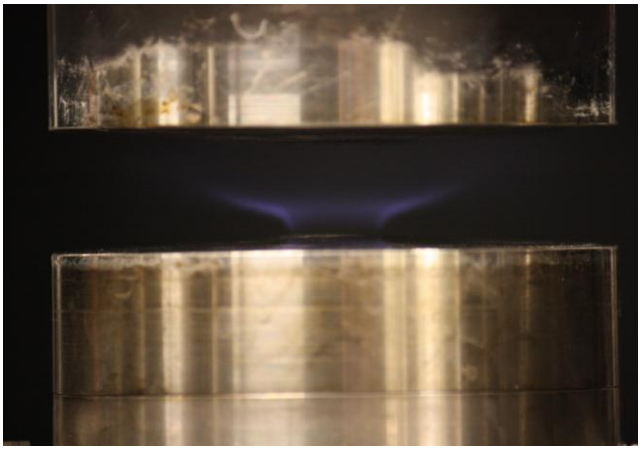

Figure 10: H_2/Air non-premixed flame at strain rate at a global strain rate of 1736 s^{-1} in the PIV-burner. The flame appears and sounds like a jet out of the fuel (bottom nozzle) side of the burner.

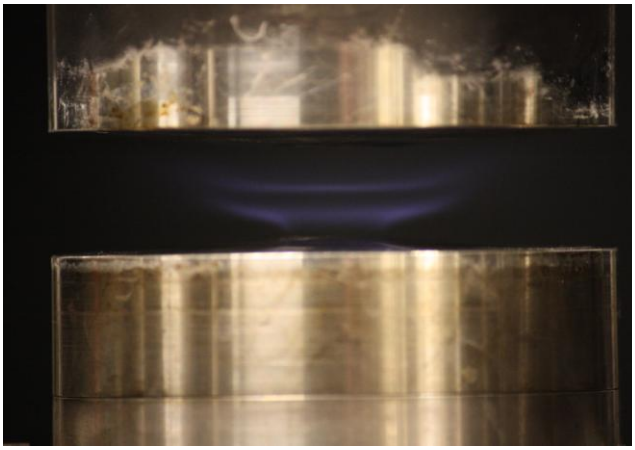

Figure 11a: H_2/Air non-premixed flame at strain rate at a global strain rate of 1350 s^{-1} in the PIV-burner. This is labeled as mode 1 and was more dominant at lower strain rates (below 1000 s^{-1}).

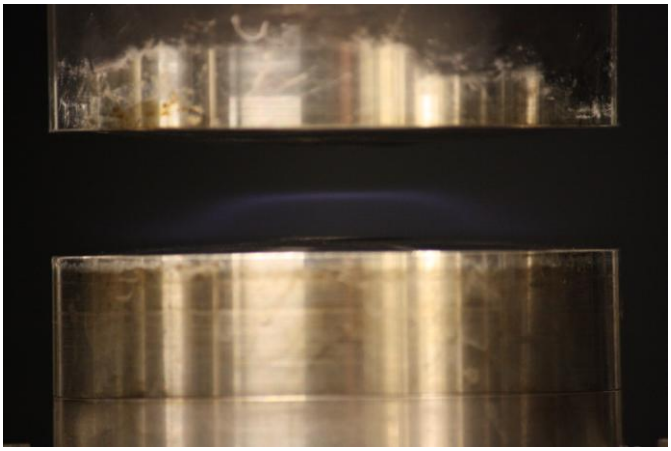

Figure 11b: H_2/Air non-premixed flame at strain rate at a global strain rate of 1350 s^{-1} in the PIV-burner. This is labeled as mode 2 and was more dominant at higher strain rates (above 1000 s^{-1}) .

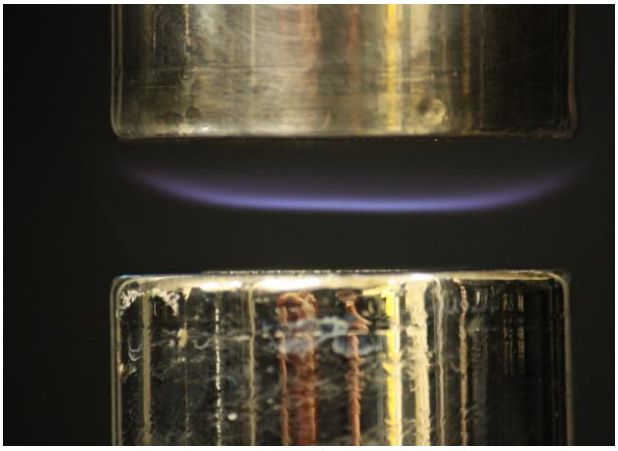

Figure 12: H_2/Air non-premixed flame in the coflow-burner at a global strain rate of 67.8 s^{-1}. The outer diameter of the burner = 5 cm.

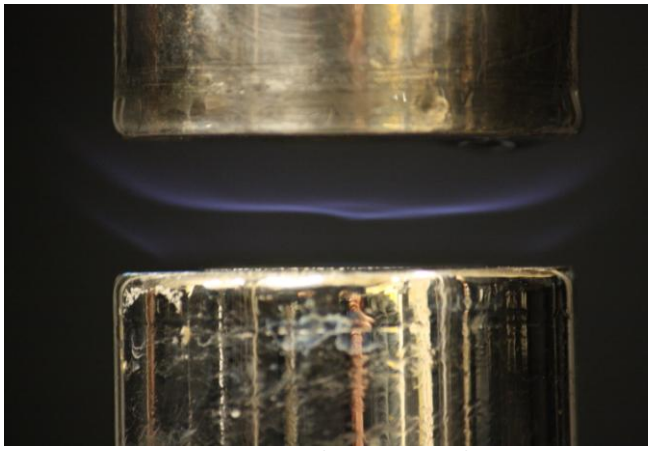

Figure 13: H_2/Air non-premixed flame in the coflow-burner at a global strain rate of 239.7 s^{-1}. This was one of the two stable modes of the flame.

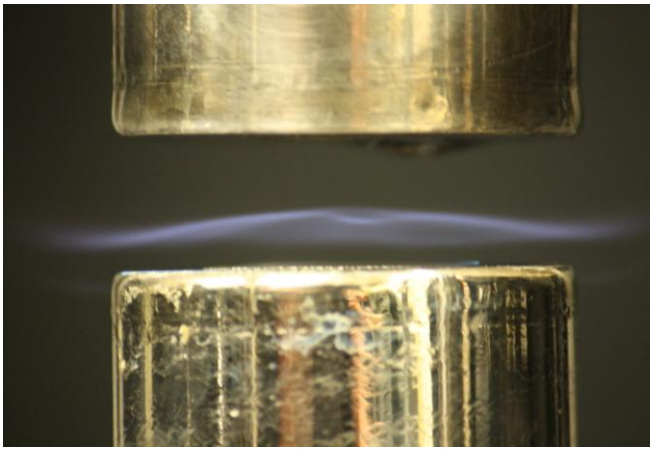

Fig 14: H_2/Air non-premixed flame in the coflow-burner at strain rate = 239.7 s^{-1}. This was second of the two stable modes of the flame.

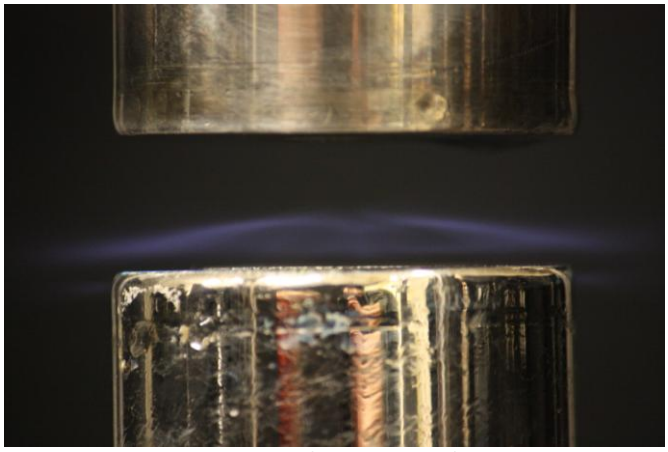

Fig 15: H_2/Air non-premixed flame in the coflow-burner at strain rate = 420.5 s^{-1}. The second mode now dominates. Notice the radial elongation of the flames.

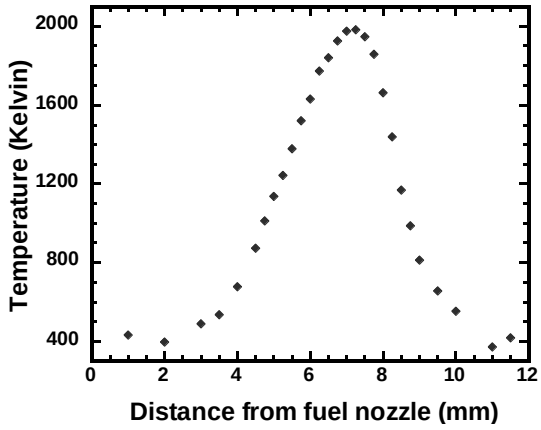

Figure 16: Temperature profile at a global strain rate of 67.8 s^{-1}.

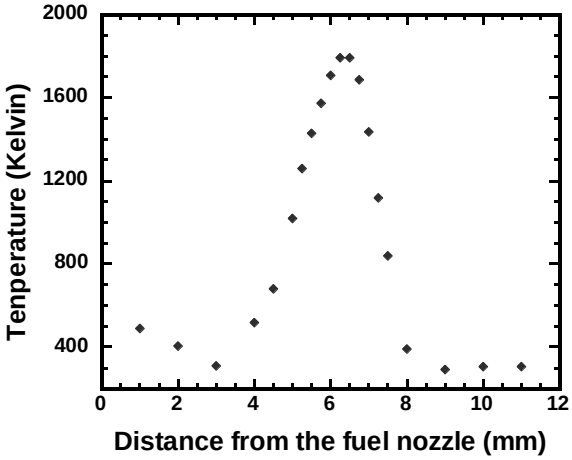

Figure 17: Temperature profile at a global strain rate of 135.7 s^{-1}.

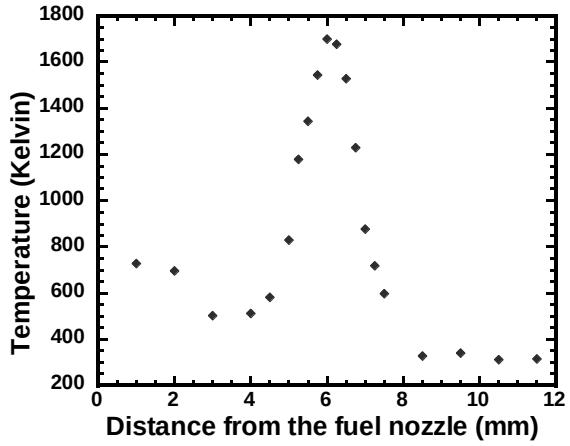

Figure 18: Temperature profile at a global strain rate of 203.5 s^{-1}

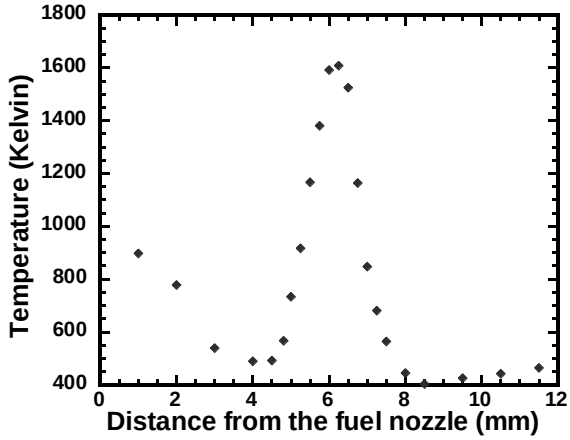

Figure 19: Temperature profile at a global strain rate of 239.7 s^{-1}

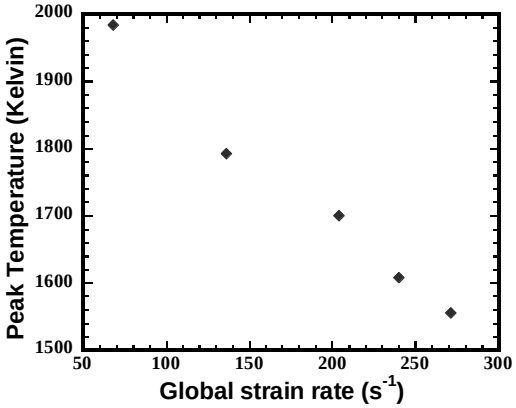

Figure 20: Peak flame temperature vs Global strain rate (s^{-1})